for this concentration is close to the solvent melting temperature.

Concluding Remarks

All of the DSC experiments are consistent with the existence of structures possessing some degree of order in the aPS–CS_2 gels. Such a conclusion is shared by other authors.[14] However, the work presented here shows that the structures responsible for the gel physical cross-links owe their existence to the formation of a stoichiometric compound.

There is virtually no molecular weight effect on the melting points determined by DSC, unlike those measured mechanically. Consequently, the values of the gel melting enthalpies as obtained from the Ferry–Eldrige equation are certainly misleading.[1] From the melting enthalpies measured here, an estimate of the amount of material participating in the links can be attempted. On an average basis of 10 cal/g (a value that represents the order of magnitude usually encountered in nonpolar organic systems) the gel would contain 5–10% of these structures. Such figures seem reasonable in view of the atactic character of this polymer, which cannot contain long stereoregular sequences. Recent statistical calculations[15] carried out to estimate the content of syndiotactic sequences possessing a subsequent length can account for the above figures.

Finally, a possible structure could resemble a ladder, the rungs of which would be the CS_2 molecules. Such a picture has been recently proposed for iPS physical gels on the basis of DSC and neutron diffraction experiments.[16] If such a model turned out to be correct, the same structures would be obtained by different mechanisms (in good solvent for aPS; in a phase-separating system for iPS).

Registry No. aPS, 9003-53-6; CS_2, 75-15-0.

References and Notes

(1) Tan, H. M.; Hiltner, A.; Moet, E.; Baer, E. *Macromolecules* **1983**, *16*, 28.
(2) Clark, J.; Wellinghoff, S. T.; Miller, W. G. *Polym. Prepr. (Am. Chem. Soc., Div. Polym. Chem.)* **1983**, *24*(2), 86.
(3) Gan, Y. S.; François, J.; Guenet, J. M.; Gauthier-Manuel, B.; Allain, C. *Makromol. Chem., Rapid Commun.* **1985**, *6*, 225.
(4) Guenet, J. M.; Willmott, N. F. F.; Ellsmore, P. A. *Polym. Commun.* **1983**, *24*, 230.
(5) Gan, Y. S.; François, J.; Guenet, J. M. *Macromolecules* **1986**, *19*, 173.
(6) The words "crystallites", "crystal", "crystallization", and the like are employed with quotation marks in order to emphasize that we may not be dealing with crystalline systems in the usual sense of the word.
(7) Boyer, R. F.; Baer, E.; Hiltner, A. *Macromolecules* **1985**, *18*, 427.
(8) Gan, Y. S.; Nuffer, R.; Guenet, J. M.; François, J. *Polym. Commun.* **1986**, *27*, 233.
(9) Lobanov, A. M.; Frankel, S. Ya *Polym. Sci. USSR (Engl. Transl.)* **1980**, *22*(5), 1150.
(10) Takahashi, A.; Sakai, M.; Kato, T. *Polym. J. (Tokyo)* **1980**, *12*(5), 335.
(11) Gauthier-Manuel, B.; Meyer, R.; Pieransky, P. *J. Phys. E: Sci. Instrum.* **1984**, *17*, 1177.
(12) Uberreiter, K.; Orthmann, H. J. *Kunststoffe* **1958**, *48*, 525.
(13) Jenckel, E.; Hensch, R. *Kolloid Z.* **1953**, *130*, 89.
(14) Domsky, R. C.; Alamo, R.; Edwards, C. O.; Mandelkern, L. *Macromolecules* **1986**, *19*, 310.
(15) Gan, Y. S.; Sarasin, D.; Guenet, J. M.; François, J. *Makromol. Chem., Rapid Commun.*, submitted.
(16) Guenet, J. M. *Polym. Bull. (Berlin)* **1985**, *14*, 105.

Self-Diffusion Measurements in Polymer Solutions at the Θ Temperature by Forced Rayleigh Light Scattering

H. Deschamps and L. Léger*

Laboratoire de Physique de la Matière Condensée, Collège de France, 75231 Paris Cedex 05, France.

Received February 14, 1986

ABSTRACT: Using forced Rayleigh light scattering technqiues (FRS), we have measured the self-diffusion coefficient, D_{self}, of polystyrene chains in cyclopentane at the Θ temperature as a function of both molecular weight M and polymer concentration c. For entangled solutions at the Θ temperature, the FRS signal shows a strong amplification as compared to the dilute, Θ, or semidilute good solvent cases. We show that this effect can be attributed to the formation in the sample of an index of refraction grating, due to monomer–photoexcited label interactions. The long-time relaxation of the FRS signal yields the self-diffusion coefficient of the labeled chains, and we obtain $D_{self} \sim M^{-2\pm0.1}c^{-3.1\pm0.2}$, in agreement with reptation and scaling predictions, assuming the tube width to be equal to the correlation length of the Θ solution, $\xi \sim c^{-1}$.

Introduction

The self-diffusion coefficient (D_{self}) of polymer chains has proven to be a quite interesting parameter to characterize individual chain motions in entangled solutions or melts.[1]

Several techniques have been used in recent years to measure D_{self},[2-8] and in the case of long enough chains in good solvent conditions, a good agreement was observed[2,9] between measurements and theoretical predictions from the reptation model[10] and the scaling approach to polymer solutions.[11,12] The case of Θ solutions, however, is far less clear from a theoretical point of view: due to the exact compensation between two-body monomer–monomer and monomer–solvent interactions, the correlation length of the monomer density is proportional to the average distance between three monomer contact points and should scale like $\xi \sim c^{-1}$.[13] However, the chains are real chains that cannot cross each other, and individual chain motions may be restricted by the two monomer contact points (average distance $d \sim c^{-1/2}$).[14] If such is the case, simple reptation arguments are not easy to develop, as they lead to a tube width, d, different from the screening length of the hydrodynamic interactions ξ.

From quasi-elastic light scattering measurements, Amis and Han[15] have obtained a characteristic time for the slow mode obeying simple scaling laws. It is not clear, however, that these slow modes may be attributed to center-of-mass translational diffusion of the chains.[16]

In order to better understand the dynamic properties of entangled Θ solutions, we have undertaken systematic

0024-9297/86/2219-2760$01.50/0

Table I
Characteristics of the Different Polystyrene Samples Used

M_w	M_w/M_n	c^*,[a] g/g
261 800	1.10	7.8×10^{-2}
657 000	1.29	4.9×10^{-2}
861 000	1.30	4.3×10^{-2}

[a] Evaluated from $c^* = 40(M_w)^{-0.5}$.[21]

measurements of D_{self} as a function of polymer molecular weight and concentration, using the forced Rayleigh light scattering technique (FRS) and the system polystyrene–cyclopentane (Θ = 23 °C).

In part I, we discuss experimental details along with the particular characteristics of the FRS signal in entangled Θ solutions. In part II, the self-diffusion data extracted from the long-time relaxation of the FRS signal are presented, and in part III, the data are discussed.

I. Experimental Section

(1) Principle of the Method. FRS is a tracer technique in which the diffusion length can be made as short as 0.5 μm. A few polymer chains in the solution are chemically labeled with photochromic molecules (one or two per chain). The photochromic molecules are photoexcited with a pulse of light having a sinusoidal spatial repartition (interference pattern), thus creating an absorption grating for any beam whose wavelength is chosen in the absorption band of the photoexcited species. If the lifetime of the photoexcited label is long compared to the diffusion of the chains over the interfringe spacing, the relaxation of the light intensity diffracted by the grating gives a direct measurement of the self-diffusion coefficient of the labeled chains.

(2) Experimental Procedure. The labeled polymer chains we use are anionically prepared and bear one photochromic spiropyran molecule at each extremity. The unlabeled chains are identical with the labeled ones except for the spiropyran molecules. Their characteristics are listed in Table I. The solutions are prepared by weighing the desired quantities of polymer and cyclopentane (spectroscopic grade) and then allowed to homogenize for more than 1 month in an oven at 40 °C under gentle intermittent agitation. They are then transferred into the measurement cell (optical path 5 mm) and cooled to 23 °C 2 days before the experiment. The temperature of the sample cell is maintained constant within ±0.05 °C during the whole experiment with an electronic temperature control.

A detailed description of the experimental setup has been given.[2] Two slight modifications have been made to increase its performance: (i) a symmetrical path interferometer is used on the exciting beam in order to allow for small interfringe spacing ($i \lesssim 1$ μm); (ii) the trigger unit now allows for measurements of the background intensity falling on the photocathode before the exciting pulse. The number of adjustable parameters in the fitting procedure is thus reduced from four to three (see the discussion of the fitting procedure in ref 2), increasing the confidence in the determination of D_{self}.

For all the experiments presented below, the concentration of labeled chains is kept well below the crossover concentration between the dilute and semidilute concentration ranges, in order to minimize the interactions between photoexcited species. The exciting UV pulse has a duration usually limited to 20 ms and an energy density less than 10 mW/mm² in order to avoid spurious thermal effects. Heating by the exciting pulse leads to distortions of the diffracted intensity vs. time curves, which are easily detected and usually appear at exciting energies more than 10 times larger than in our working conditions. Care has also been taken to avoid heating of the sample by the reading beam, which is attenuated to 7×10^{-6} W.

(3) "Anomalous" FRS Signal in Entangled Θ Solutions. Figure 1 shows typical diffracted intensity vs. time curves for both a dilute (a) and a semidilute (b) polymer solution at the Θ temperature. Curve 1a represents a usual FRS signal: the diffracted intensity increases during the exciting pulse and then relaxes as soon as the excitation has stopped. On the contary, the signal on curve 1b is "anomalous": it continues to increase long after (a few tenths of a second) the exciting UV pulse has stopped, and

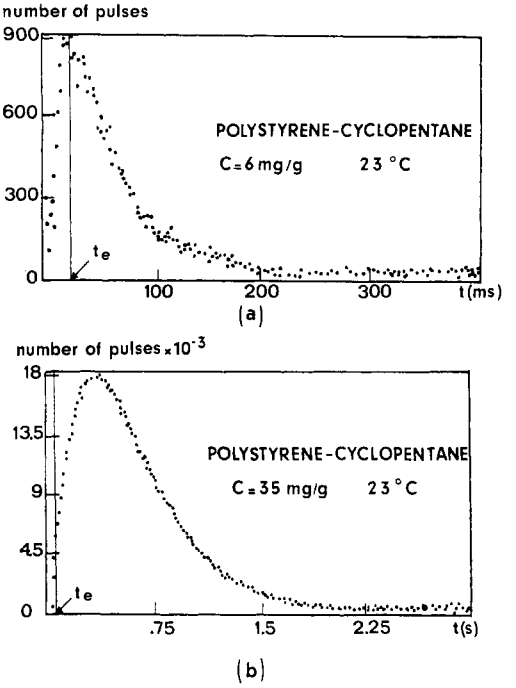

Figure 1. Typical FRS diffracted intensity vs. time curves for polystyrene end-labeled with spiropyran in cyclopentane at 23 °C: curve a, dilute regime (the FRS signal increases during the photoexciting pulse (duration τ_e)); curve b, semidilute regime (the FRS signal continues to increase long after τ_e, and its maximum is about 10 times larger for similar excitation conditions and number of labels than in curve a).

the maximum diffracted intensity is about 10 times larger than in curve 1a for comparable excitation conditions and number of labeled molecules. The shape of curve 1b remains unchanged when the interfringe spacing is varied. Such an anomalous FRS signal has already been reported by Wesson et al.[17] in the case of rather concentrated polystyrene–cyclohexane solutions at the Θ temperature, but without any analysis of the conditions under which this slowly increasing signal appeared or discussion of its possible origin. On the other hand, Johnson[18] has attributed similar FRS signals obtained with small probes or labeled protein solutions to the presence of several species (photoexcited and nonphotoexcited, or isolated probes and labeled proteins) having different hydrodynamic characteristics and giving rise to two independently relaxing gratings initially out of phase. For the polymer solutions we have studied, we have observed a behavior analogous to curve 1b in various systems close to the Θ temperature (polystyrene–cyclopentane between 20 and 40 °C, polystyrene–cyclohexane close to 35 °C, and polystyrene–*trans*-decalin at room temperature) for large enough concentrations, but the anomalous signal never shows up for low concentrations or for benzene, toluene, or tetrahydrofuran solutions. It cannot be attributed to a modification of the photochromic properties of the spiropyran label: Figure 2 gives the photochromic characteristics of the labeled chains (visible absorption spectra under UV irradiation (λ_{exc} = 350 nm) and relaxation rate of the open form at λ = 632.8 nm) for both cyclopentane and benzene solutions. In Figure 3a we report the intensity transmitted through a solution that shows an anomalous FRS signal immediately after a photoexciting UV pulse (without interference fringes). The absorbance of the sample at 632.8 nm does not display any anomalous kinetics: it decreases immediately after the excitation has ceased. Moreover, we have obtained a FRS signal completely analogous to the one of Figure 1b (same diffraction efficiency and comparable kinetics) on the same sample, replacing the He–Ne reading laser by a He–Cd laser, whose wavelength, λ = 442 nm, is out of the absorption band of the sample (see Figure 2). This clearly demonstrates that the signal of Figure 1b is not due to the absorption grating printed in the sample by the exciting UV pulse. Indeed, it is well-known that usually both absorption and phase gratings are produced simultaneously in a FRS experiment. One contribution to the phase grating is due to the thermally

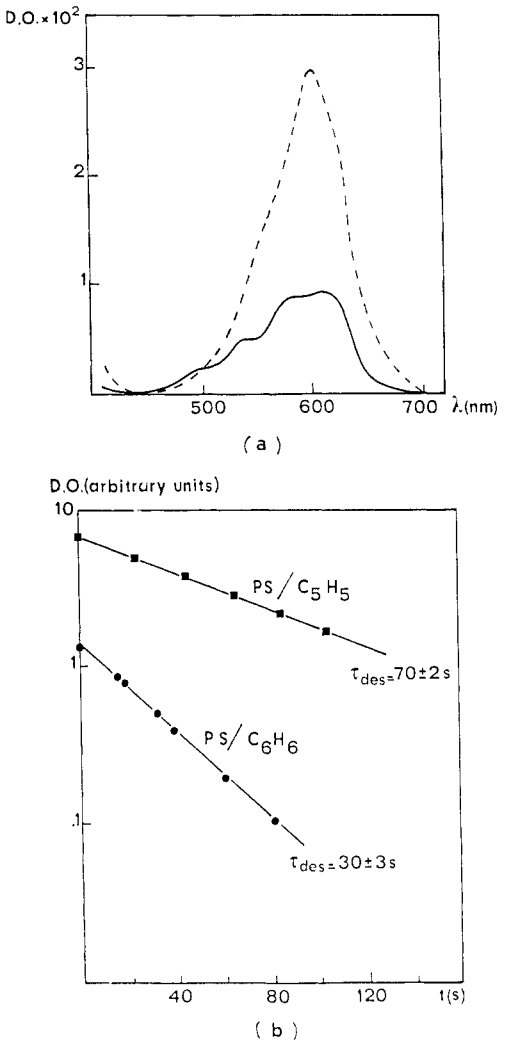

Figure 2. (a) Visible absorption spectra of the labeled polymer (M_w = 14 000) under UV excitation (λ = 350 nm) for (- - -) cyclopentane solution (c = 0.6 mg/g, P_{exc} = 16 mW/cm²) and (—) benzene solution (c = 0.6 mg/g, P_{exc} = 6 mW/cm²). (b) Characterization of the deexcitation rate of the photoexcited chains monitored at λ = 632.8 nm for the two systems of curve a.

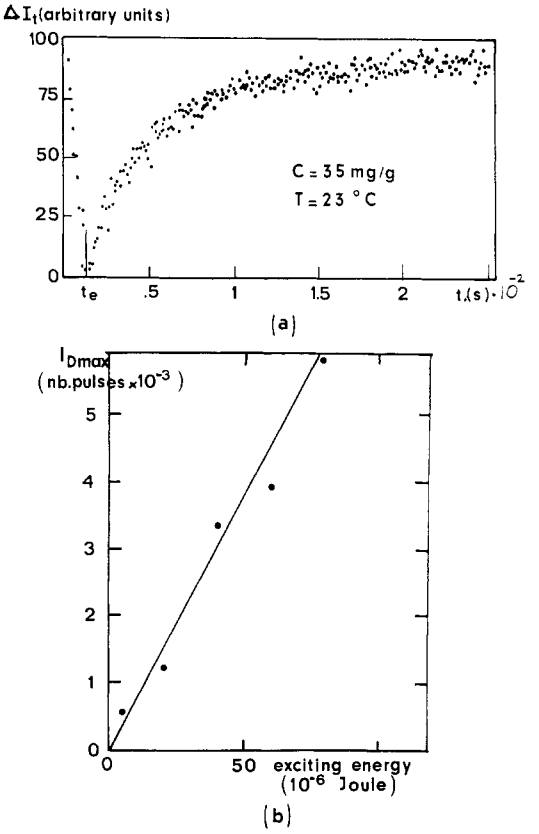

Figure 3. Variation of the transmitted intensity at λ = 632.8 nm through a sample showing an anomalous kinetics for the FRS signal (M_w = 861 000, c = 35 mg/g in cyclopentane at 23 °C) after a UV exciting pulse without interference fringes. The absorption of the sample does not show any anomalous kinetics. (b) Diffraction efficiency $I_{D,max}$ as a function of the exciting energy.

induced modulation of the index of refraction of the sample always associated with the absorption of the exciting radiation. Such a thermally induced grating has been widely used to measure thermal diffusivity[19,20] and relaxes very rapidly as the thermal diffusivity is usually of order of 10^{-3}–10^{-4} cm²/s. Another contribution to the phase grating is due to the modification of the index of refraction associated with the presence of the photoexcited label, as an absorption band always implies anomalous dispersion. However, as clearly demonstrated by Fayer et al.,[21] the relative contribution of the two kinds of gratings associated with one absorption band (phase and absorption) depends on the position of the reading wavelength λ_R with respect to the wavelength of maximum absorbance of the photoexcited species. For $\lambda_R = \lambda_{max}$, the diffraction is due to a pure absorption grating, while for λ_R corresponding to the half-width of the absorption spectra, the phase grating contribution reaches a maximum and then decreases toward the wings of the spectra more slowly than the absorption grating contribution. The fact that we observe a diffraction efficiency independent of the reading wavelength for two wavelengths located either at the half-width of the absorption band or out of it strongly suggests that the index of refraction grating predominantly responsible for the difffraction we detect is not related to anomalous dispersion associated with the photoexcited label. This hypothesis is further supported by the linearity of the diffraction efficiency as a function of the concentration of the photoexcited species reported in Figure 3b: for an index of refraction grating, one expects a diffracted intensity $I_D \sim I_0 \sin^2(\pi l \Delta n/(2\lambda \cos\theta'))$; i.e., for small arguments,[22] $I_D \sim I_0 \Delta n^2 (\pi l/(2\lambda \cos\theta'))^2$ (l is the sample thickness and θ' the angle of the beam with the grating plane). If the modulation of the index of refraction responsible for the diffraction was due to anomalous dispersion, one would expect $\Delta n \sim c_{photoex}$ and I_D quadratic in exciting energy. Indeed, the normal FRS signal of Figure 1a can be quantitatively accounted for by comparable absorption and phase gratings: for the conditions of the experiment ($c_{label} \sim 10^{-7}$ g/g and 10 mW/mm² excitation pulse of 20-ms duration) and using the spectroscopic characteristics of Figure 2, we expect an absorbance modulation $\Delta\alpha \sim 10^{-4}$, leading to a diffracted intensity[22] $I_D \sim I_0(\sinh^2[\pi l \Delta\alpha/(4\cos\theta')]) \sim 10^{-7} I_0$, in good agreement with the data of Figure 1a, but not compatible with the 10 times enhanced signal of Figure 1b.

An important question is then to find the origin of such an index of refraction modulation. It cannot be due to thermal heating during the exciting pulse. Such heating should lead to a phase grating appearing and relaxing much faster, as the thermal diffusivity coefficient is of the order of 10^{-3}–10^{-4} cm²/s. The slow increase of the signal of Figure 1b rather suggests that this phase grating has to be related with a progressive formation of a modulation of the polymer concentration. With $dn/dc \sim 0.1$, an amplitude of order 10^{-6} for this modulation should be sufficient to explain quantitatively the anomalous signal of Figure 1b. As the phase grating appears as a consequence of the photoexciting pulse, we think that it may be due to a local modification of the solvent quality in the regions of the sample where the highly polar photoexcited molecules have been formed and subsequently to a local modification of the polymer concentration. It has indeed already been reported that photoexcited spiropyran molecules, at concentrations much higher than in the present study, could lead to polymer precipitation.[23] Unfortunately, in our experimental conditions we do not have sensitive enough techniques to detect independently the presence of such a small concentration modulation. If we assume that the above-proposed mechanism is the correct one, the long-time relaxation of the polymer concentration modulation is driven by the relaxation of the periodic

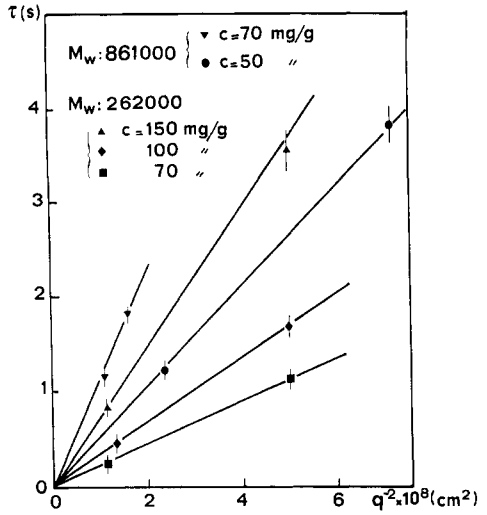

Figure 4. Evolution of the long-time relaxation rate of the FRS signal for different polystyrene–cyclopentane solutions as a function of the water vector $q = 2\pi/i$, with i the interfringe spacing. The linear behavior of τ vs. q^{-2} demonstrates that the relaxation of the FRS signal is due to a diffusive process.

repartition of the photoexcited molecules, i.e., by the diffusion of the labeled chains over the interfringe spacing. The long-time relaxation of the anomalous FRS signal thus yields the self-diffusion coefficient of the chains.

II. Results

We have analyzed the long-time decrease of the diffracted intensity in a way similar to that discussed in ref 2, except for the background intensity, which was no longer adjusted. In all cases we have been able to describe the data with a single relaxation time τ. A typical dependence of the relaxation time τ as a function of the inverse of the square of the wave vector $q^{-2} = (2\pi/i)^{-2}$, with i the interfringe spacing, is reported in Figure 4. The linear behavior observed when the relaxation time τ is short compared to the photoexcited lifetime of the spiropyran molecule, $\tau_{des} \sim 70$ s, demonstrates that we are indeed dealing with a diffusion process.

In Figure 5 the corresponding diffusion coefficients, $D_{self} = 1/\tau q^2$, are reported, on logarithmic scales, as a function of the polymer concentrations, c. D_{self} monotonously decreases with c, and for high enough concentrations, a linear behavior is observed, corresponding to a power law $D_{self} \sim c^{-3.1\pm0.2}$.

In Figure 6 we report, again on logarithmic scales, the molecular weight dependence of D_{self} for two rather high concentrations, $c_1 = 150$ mg/g and $c_2 = 200$ mg/g. In both cases the power law $D_{self} \sim M^{-2\pm0.1}$ is well obeyed.

As it is now well-known that tube renewal effects may contribute to self-diffusion,[9,24,25] we have checked the dependence of the measured diffusion coefficient (labeled chain index of polymerization N) on the molecular weight of the unlabeled chains (index of polymerization P). Keeping the labeled chain concentration constant and less than $c^*(N)$ and varying the overall polymer concentration in the range 70–150 mg/g, we have observed for $N = 8610$ a 25% decrease of the diffusion coefficient for P going from 8610 to 28 000, a variation significantly smaller than in the good solvent case.[9] In the explored concentration range, the concentration dependence of the diffusion coefficient was apparently independent of the molecular weight of the matrix.

III. Discussion

The dynamic properties of semidilute Θ solutions have been worked out theoretically by Brochard and de Gennes.[13,14] They appear far more delicate than for good solvent solutions. The essential difficulty comes from the two length scales, average distance between three-body contact points and average distance between two-body contact points, which both play a role in chain dynamics and elasticity.[13,14,26] In order to transpose reptation ideas to the Θ-solvent case, one has to examine in detail the physical significance of those two lengths in order to know which one corresponds to the topological constraints applied on the test chain by its neighbors, i.e., which one governs the tube size.

In the dilute Θ regime, the chains are characterized by their radius of gyration, $R_G \sim N^{1/2}a$ (a and N are the size and the number of the statistical units of the chain). As the monomer–monomer interactions vanish at Θ, each chain contains a number of self-knots proportional to $N^{1/2}$.[13] The chains are Gaussian, and the average distance between two successive self-entanglements is $l_{p_0} \sim N^{1/4}a$. For concentrations greater than $c^* \sim N/R_G^3 \sim N^{-1/2}$, the chains start to overlap. Three-body contact points start to form in appreciable quantity. Their average distance, ξ, which is the screening length for both static and hydrodynamic interactions,[13] scales like $\xi \sim R_G(c/c^*)^{-1}$. If

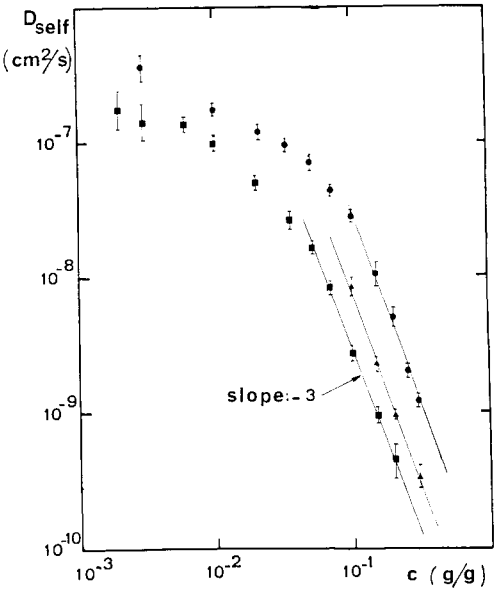

Figure 5. Concentration dependence of the self-diffusion coefficient D_{self} deduced from the long-time relaxation rate of the FRS signal for three different molecular weights: (●) M_w = 262 000; (▲) M_w = 657 000; (■) M_w = 861 000.

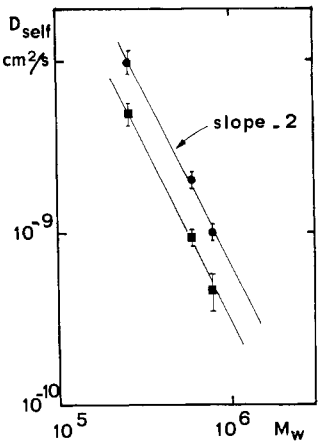

Figure 6. Molecular weight dependence of the self-diffusion coefficient D_{self} for two different concentrations: (●) c_1 = 150 mg/g; (■) c_2 = 200 mg/g.

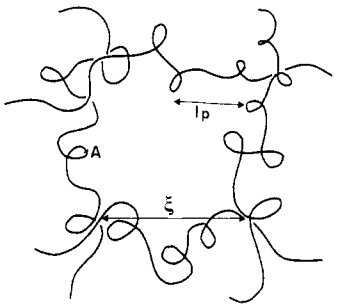

Figure 7. Schematic representation of a semidilute Θ system: $\xi \sim c^{-1}$ is the screening length for static and hydrodynamic interactions. It corresponds to the average distance between three monomer contact points. Inside a volume ξ^3 we have essentially one self-entangled chain (average distance between two monomers contact points $l_p \sim c^{-1/2}$). We can thus assume a tube width proportional to ξ.

g is the number of monomers in a volume ξ^3, we have $g = c\xi^3 \sim c^{-2}(R_G c^*)^3$; i.e., $\xi \sim g^{1/2}a$. This last relation means that, in the volume ξ^3, on the average, all the monomers pertain to the same chain. The average distance between binary contact points l_p scales like $l_p \sim l_{p_0}(c/c^*)^{-1/2}$ (corresponding to an average number of monomers n_p, with $n_p c a^3 = 1$). l_p and g are thus related through $l_p \sim g^{1/4}a$: inside one subunit of size ξ, we have essentially one ideal chain of g monomers, containing $g^{1/2}$ self-entanglements, as schematically presented in Figure 7. If this picture of the semidilute Θ regime is correct, it is natural to develop reptation arguments assuming a tube width proportional to ξ, as starting from one monomer on the test chain (such as A in Figure 7), we essentially meet the other chains at distances $r \sim \xi$. We can define the curvilinear diffusion coefficient of the test chain along its tube in a way completely similar to the good solvent case:[2]

$$D_t \sim \frac{kT}{\eta_s (N/g)\xi} \tag{1}$$

We thus have

$$D_t T_R \sim L_t^2 \sim (N/g)^2 \xi^2 \tag{2}$$

and

$$D_{self} T_R \sim R_G^2 \sim Na^2 \tag{3}$$

with T_R the time it takes the chain to renew its ternary contact points. Equations 2 and 3 lead to expressions for T_R and D_{self} analogous to the good solvent case:

$$T_R \sim \frac{\eta_s}{kT}\left(\frac{N}{g}\xi\right)^3 \tag{4}$$

$$D_{self} \sim \frac{kT}{\eta_s \xi (N/g)^2} \tag{5}$$

With $\xi \sim c^{-1}$ and $g \sim c^{-2}$, we obtain

$$D_{self} \sim N^{-2} c^{-3} \tag{6}$$

Equation 6 is in surprisingly good agreement with our experimental results presented on Figures 5 and 6, giving thus strong experimental support to the picture of the entangled Θ regime schematically presented in Figure 7. The analogy with the good solvent case seems straightforward, but one has to notice that T_R does not characterize the same process in both cases: in a good solvent, T_R is the time required by the chain to renew its configuration, i.e., to change all its entanglements, while in the Θ-solvent case, T_R is associated with the renewal of the contact points of the test chain with its neighbors and not with the renewal of its own self-entanglements. Anyway, in both cases T_R represents the temporal limit between liquid-like and elastic behavior: if a constraint is applied with a frequency larger than T_R^{-1}, the constraint is transmitted to the subunits of size ξ, which in the case of a Θ solvent respond with an elastic modulus characteristic of the "microgel"[14] formed by the self-entangled portion of the chain.

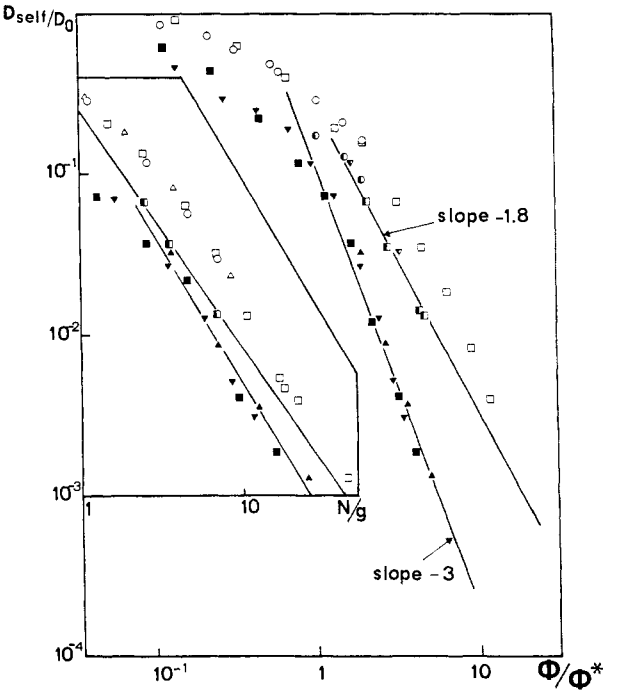

Figure 8. Evolution of the reduced diffusion coefficient D_{self}/D_0 as a function of the reduced polymer volume fraction ϕ/ϕ^* for both Θ and good solvent conditions (respectively full and open symbols). In both cases we obtain universal curves, illustrating the validity of the scaling description for macroscopic, long-time chain dynamics. Half-filled symbols correspond to good solvent solutions, with unlabeled chains much longer than the labeled one, i.e., to pure reptation. In the insert the same data are reported in terms of the number of topological constraints along the test chain, N/g.

From the above analysis we can understand why the self-diffusion coefficient is less sensitive to the motion of the surrounding chains (tube renewal) in a Θ solvent. For a tube renewal process driven by the reptation of the surrounding chains, we expect an effective diffusion coefficient $D_{self} = D_{rept}[1 + \alpha(N/g)^2]$.[9,27] With $g/N \sim (c/c^*)^{-2}$, the correcting term decreases much more rapidly with increasing concentrations than in the good solvent case $[g/N \sim (c/c^*)^{-5/4}]$.

We have summarized our results in Figure 8, where the reduced diffusion coefficient D_{self}/D_0 is reported (full symbols) on logarithmic scales as a function of the reduced polymer volume fraction ϕ/ϕ^*. D_0 is the diffusion coefficient in the zero concentration limit, evaluated from sedimentation and quasi-elastic light scattering data.[26,28] The polymer volume fraction ϕ has been evaluated by using partial specific volumes from ref 29, and ϕ^* values have been deduced from the scaling law $\phi^* \sim 40 M_w^{-1/2}$.[26] The universal curve illustrates the validity of the scaling approach presented above. For comparison, our good solvent data of ref 2 and 9 (open and half-filled symbols) are reported in the same corresponding reduced units. Universal scaling laws are also observed in good solvent, but a simple power law dependence corresponding to the predicted reptation exponent −1.8 is only obtained when

the motion of the matrix unlabeled chains is frozen (half-filled symbols).[9] In the insert the same data are reported as a function of the number of entanglements along the test chain, $N/g \sim (\phi/\phi^*)^x$, with $x = -5/4$ for good solvent and $x = -2$ for Θ solvent. We do not expect exactly the same scaling law for the two solvents due to the different molecular weight dependences of D_0, but the fact that the data points fall very close in good and Θ solvent gives a good illustration of the fact that the relevant parameter for self-diffusion is the number of topological constraints imposed on the test chain by its neighbors.

Conclusion

Using the forced Rayleigh light scattering technique, we have measured the self-diffusion coefficient of polystyrene chains in cyclopentane at the Θ temperature. Both the molecular weight and the concentration dependences we obtain are in good agreement with a description of semidilute Θ solutions based on reptation and scaling ideas: (i) the M^{-2} behavior and the weak dependence of D_{self} on the molecular weight of the unlabeled chains are characteristic of a reptative process; (ii) the c^{-3} dependence can be interpreted by assuming that the virtual tube inside which each test chain is confined by its neighbors has a width proportional to the average distance between ternary monomer contacts, $\xi \sim c^{-1}$. This seems a priori surprising: one is used to thinking of tube width in terms of average distance between binary monomer contact points, as the chains cannot cross each other. However, a careful analysis of the description of entangled Θ systems proposed by Brochard and de Gennes shows that this results from the fact that, on the average, all the monomers contained in one subunit of size ξ pertain to the same chain. As far as we are dealing with slow macroscopic motions (i.e., over distances greater than the chain radius), our results show that semidilute Θ systems obey simple scaling laws very similar to those of the good solvent case.

Registry No. Polystyrene, 9003-53-6; cyclopentane, 287-92-3.

References and Notes

(1) de Gennes, P.-G.; Lêger, L. *Annu. Rev. Phys. Chem.* **1982**, *33*, 49.
(2) Lêger, L.; Hervet, H.; Rondelez, F. *Macromolecules* **1981**, *14*, 1732.
(3) Callaghan, P. T.; Pinder, D. N. *Macromolecules* **1980**, *13*, 1085. Callaghan, P. T.; Pinder, D. N. *Macromolecules* **1981**, *14*, 1334.
(4) Tanner, J. E. *Macromolecules* **1971**, *4*, 748.
(5) Klein, J.; Briscoe, B. J. *Proc. R. Soc. London Ser. A*, **1979**, *365*, 53.
(6) Hanley, B.; Balloge, S.; Tirrell, M. *Chem. Eng. Commun.* **1983**, *24*, 93.
(7) Martin, J. E. *Macromolecules* **1984**, *17*, 1279.
(8) Bartels, C. R.; Crist, B.; Graessley, W. W. *Macromolecules* **1984**, *17*, 2702.
(9) Marmonier, M. F.; Lêger, L. *Phys. Rev. Lett.* **1985**, *55*, 1078.
(10) de Gennes, P.-G. *J. Chem. Phys.* **1971**, *55*, 572.
(11) de Gennes, P.-G. *Scaling Concepts in Polymer Physics*; Cornell University: Ithaca, NY, 1979.
(12) de Gennes, P.-G. *Macromolecules* **1976**, *9*, 594.
(13) Brochard, F.; de Gennes, P.-G. *Macromolecules* **1977**, *10*, 1157.
(14) Brochard, F. *J. Phys. (Les Ulis, Fr.)* **1983**, *44*, 39.
(15) Amis, E. J.; Han, C.; Matsushita, Y. *Polymer* **1984**, *25*, 650.
(16) Balloge, S.; Tirrell, M. *Macromolecules* **1985**, *18*, 817.
(17) Wesson, J. A.; Noh, I.; Kitano, T.; Yu, H. *Macromolecules* **1984**, *17*, 782.
(18) Johnson, C. S. *J. Opt. Soc. Am.* **1985**, *B2*, 317.
(19) Eichler, H.; Saije, G.; Stahl, H. *Appl. Phys.* **1973**, *44*, 5383.
(20) Phol, D. W.; Schwatz, S. E.; Irniger, V. *Phys. Rev. Lett.* **1973**, *31*, 32.
(21) Nelson, K. A.; Casalegno, R.; Bwagne-Miller, R. J.; Fayer, M. D. *J. Chem. Phys.* **1982**, *77*, 1144.
(22) Glass, A. H. In *Photonics*; Balkanski, H., Lallemand, P., Eds.; Gauthier-Villars: Paris, 1975.
(23) Irie, M.; Tanaka, H. *Macromolecules* **1983**, *16*, 210. Menju, A.; Hayashi, K.; Irie, M. *Macromolecules* **1981**, *14*, 755.
(24) Green, P. F.; Mills, P. J.; Palmstrøm, C. J.; Mayer, J. W.; Kramer, E. J. *Phys. Rev. Lett.* **1984**, *53*, 2145.
(25) Smith, B. A.; Samulski, E. T.; Yu, L. P.; Winnik, M. A. *Phys. Rev. Lett.* **1984**, *52*, 45.
(26) Adam, M.; Delsanti, M. *Macromolecules* **1985**, *18*, 1760.
(27) Daoud, M.; de Gennes, P.-G. *J. Polym. Sci., Polym. Phys. Ed.* **1979**, *17*, 1981.
(28) Vidakovic, P.; Allain, C.; Rondelez, F. *J. Phys., Lett.* **1981**, *42*, L-323.
(29) Pouyet, G.; Candau, F.; Dayantis, J. *Makromol. Chem.* **1976**, *177*, 2973.

Upper and Lower Critical Solution Temperature Behavior in Thermoplastic Polymer Blends

Guangmin Cong,† Yuhui Huang,† William J. MacKnight,* and Frank E. Karasz

Polymer Science and Engineering Department, University of Massachusetts, Amherst, Massachusetts 01003.

Received March 3, 1986

ABSTRACT: The phase behavior of blends of polystyrene ($\bar{M}_w$ = 115 000, M_w/M_n < 1.06) (PS_{115}) and a random copolymer of carboxylated poly(2,6-dimethyl-1,4-phenylene oxide) (C^y-PPO) has been studied by differential scanning calorimetry (DSC) and light scattering. In C^y-PPO, y represents the carboxyl content (COOH mole percent). The phase diagrams of $C^{8.0}PPO/PS_{115}$ and $C^{10.3}PPO/PS_{115}$ were found to exhibit both UCST (upper critical solution temperature) and LCST (lower critical solution temperature) behavior. The phase behavior is reversible. The miscible region between the UCST and LCST decreases with increasing carboxyl content in the C-PPO, and the critical point moves to lower mass fraction of copolymer. In the blends $C^{4.5}$-PPO/PS_{115} and $C^{6.7}$-PPO/PS_{115} no phase separation was observed during thermal treatment. The results obtained from both DSC and light scattering are consistent.

Introduction

The phase behavior of solutions at constant pressure and temperature is governed by the Gibbs free energy of mixing ΔG_m:

$$\Delta G_m = \Delta H_m - T\Delta S_m \quad (1)$$

Using the Flory–Huggins theory,[1] one may write the entropy of mixing ΔS_m as

$$\Delta S_m = -R(n_1 \ln \phi_1 + n_2 \ln \phi_2) \quad (2)$$

where n_i is the number of moles of component i with volume fraction ϕ_i. For a system where there are no

† Permanent address: Department of Chemistry, Zhong-Shan University, Guangzhou, People's Republic of China.

0024-9297/86/2219-2765$01.50/0